

**Strain dependencies of energetic, structural, and polarization properties in tetragonal  $(\text{PbTiO}_3)_1/(\text{SrTiO}_3)_1$  and  $(\text{BaTiO}_3)_1/(\text{SrTiO}_3)_1$  superlattices: a comparative study with bulks**

Yanpeng Yao and Huaxiang Fu

*Department of Physics, University of Arkansas, Fayetteville, Arkansas 72701, USA*

(Dated: August 14, 2018)

**Abstract**

First-principles density functional calculations are performed to investigate the interplay between inplane strains and interface effects in  $1\times 1$   $\text{PbTiO}_3/\text{SrTiO}_3$  and  $\text{BaTiO}_3/\text{SrTiO}_3$  superlattices of tetragonal symmetry. One particular emphasis of this study is to conduct side-by-side comparisons on various ferroelectric properties in short-period superlattices and in constituent bulk materials, which turns out to be rather useful in terms of obtaining valuable insight into the different physics when ferroelectric bulks form superlattices. The various properties that are studied in this work include the equilibrium structure, strain dependence of mixing energy, microscopic ferroelectric off-center displacements, macroscopic polarization, piezoelectric coefficients, effective charges, and the recently formulated  $\vec{k}_\perp$ -dependent polarization dispersion structure. The details of our findings are rather lengthy, and are summarized in Sec. IV.

PACS numbers: 77.84.-s, 77.80.bn, 77.80.-e

## I. INTRODUCTION

Ferroelectric (FE) materials have found spread applications in microelectronics such as sensors, actuators, transducers, etc.[1] In recent years, ferroelectric superlattices have attracted attention for their promising potential in modifying and tuning the structural and polarization properties of FE materials. For instance, when forming superlattices with BaTiO<sub>3</sub>, incipient SrTiO<sub>3</sub> was found to exhibit strong ferroelectricity.[2] Meanwhile, FE superlattices grown with desired constituents and/or periodicity provide an important field to probe and understand the fundamental physics of ferroelectric materials and related properties.[3] Among various FE superlattices, those with ultrashort period are of particular interest, since the strong interface effect may lead to some properties in the superlattices that are drastically different from those in bulk constituents. In short-period FE superlattices, one component significantly influences another, making the material properties interesting and less predictable.

In the study of FE physics, another subfield of importance is to understand the strain dependence of FE properties. Inplane strain, caused by either lattice mismatch or external stress, alters the interatomic interaction in an anisotropic manner, which often gives rise to new physics and/or phenomena. For example, inplane strains have been shown to change the critical temperature of BaTiO<sub>3</sub> by as large as 500<sup>0</sup>C.[4] Furthermore, different FE materials were found to possess very different polarization responses to inplane strain.[5, 6] While polarizations in BaTiO<sub>3</sub> and PbTiO<sub>3</sub> were found sensitive to lattice mismatch,[5] Pb(ZrTi)O<sub>3</sub> nevertheless displays a surprisingly weak polarization dependence on the inplane strain.[6] More recently, it was theoretically demonstrated that when FEs are under large strains, the  $\chi$  polarization is to saturate, and this polarization saturation was shown to be a general phenomenon applicable for different materials.[7] This finding also leads to a nature explanation on why polarization in some FEs (not the others) displays a weak strain dependence, since the polarization in these FEs is approaching the saturation and thus is less affected by the inplane strain.[7] While the strain influences on bulk FEs are amply studied, the strain-induced effects in FE superlattices are relatively less understood, however.

In this paper we intend to address a topic which concerns both of the above two subfields (namely, FE short-period superlattices as well as strain effects), by studying the property changes caused by epitaxial inplane strains in ferroelectric PbTiO<sub>3</sub>/SrTiO<sub>3</sub> and

BaTiO<sub>3</sub>/SrTiO<sub>3</sub> superlattices with short periodic length. The topic is of interest for the following reason. In short-period superlattices, the interface plays a far more important role than in long-period superlattices and in bulk, and consequently, will significantly alter the structural and polarization responses to external inplane strains. The interplay—caused by strongly interacting interface and inplane strains—makes the strain effects in short superlattices to differ from their bulk constituents and to be potentially much more complex. The above viewpoint emphasizes the differences between FE superlattices and FE bulks. On the other hand, FE superlattices must bear some resemblance to the FE bulks, since superlattices are made of individual bulk constituents. The strain responses of the superlattices thus must, to a varied degree, reflect and resemble the properties of bulk constituents. Based on these considerations, one key purpose of this work is to conduct a side-by-side comparative study of strain-induced effects in short-period FE superlattices and in FE bulks.

The advantage of a comparative study is rather obvious: by comparing bulks (with no interface) and short-period superlattices with strong interface, one is able to obtain a direct insight and understanding on the interplay of interface effect and strain effect, and on how the existence of one component in superlattices affects the other component under different inplane strains. This being said, the comparative study nevertheless is not as straightforward as it seems to be, for the following reasons. (i) In certain short-period superlattices, the rotation instability of oxygen octahedral may exist.[8, 9] On the other hand, bulk PbTiO<sub>3</sub> has only one stable phase of tetragonal symmetry without oxygen rotation as shown by the lack of soft modes at the zone boundary [10], and consideration of other phases in superlattices makes it difficult to conduct a side-by-side comparison on strain effects between superlattices and bulks. (ii) Properties such as ferroelectric off-center displacements, effective charges, and polarization structure depend on structural symmetry. By allowing rotation instability, most of properties in bulks and in superlattices can not be directly compared, and the advantage of comparative study will be largely lost. To enable a comparative study, we thus deliberately confine ourself to FE superlattices and bulks of tetragonal symmetry without oxygen rotation. For readers who are interested in superlattices with structural phases other than tetragonal symmetry, results can be found in previous reports.[8, 9, 11, 12] Experimentally, superlattices of tetragonal symmetry without oxygen rotation can be realized in several possible ways: (1) One can grow short-period superlattice films between metallic electrodes possessing no oxygen rotation. The lack of oxygen rotation in electrodes

will inhibit the rotation instability in the superlattices. (2) One may use compressive inplane strains to suppress the rotation instability. It was shown in SrTiO<sub>3</sub> that under sufficiently large inplane strain, the structure with rotation instability becomes less stable and eventually disappears.[7] (3) One may engineer superlattices by choosing atoms of different sizes to weaken the rotation instability. For instance, the rotation instability in BaTiO<sub>3</sub>/SrTiO<sub>3</sub> is considerably weaker than in PbTiO<sub>3</sub>/SrTiO<sub>3</sub>.

In this study, we apply first-principles density functional theory (DFT) calculations to 1×1 PbTiO<sub>3</sub>/SrTiO<sub>3</sub> (PT/ST) and BaTiO<sub>3</sub>/SrTiO<sub>3</sub> (BT/ST) superlattices, as well as to the individual bulk constituents PbTiO<sub>3</sub> (PT), SrTiO<sub>3</sub> (ST), and BaTiO<sub>3</sub> (BT). As shown below, various properties are to be investigated, which include microscopic ferroelectric off-center displacements, macroscopic polarization, piezoelectric coefficients, effective charges  $Z^*$ , and the recently formulated  $\vec{k}_\perp$ -dependent polarization dispersion structure [13]. A number of interesting differences between strain effects in superlattices and those effects in bulks have been found, the details of which are summarized in Sec.IV.

## II. THEORETICAL METHOD

We use first-principles density functional theory within the local density approximation[14] (LDA) to determine the structure response to external strains in superlattices and in bulks. For the 1×1 superlattices, each unit cell consists of 10 atoms. The system of tetragonal symmetry has lattice vectors  $\mathbf{a}_1$ ,  $\mathbf{a}_2$ , and  $\mathbf{a}_3$ , with  $|\mathbf{a}_1| = |\mathbf{a}_2| = a$  and  $|\mathbf{a}_3| = c$ . The optimized cell structure and atomic positions are obtained by minimizing the total energy. More specifically, for each inplane lattice constant  $a$ , the out-of-plane  $c$  length and atomic positions are optimized. Biaxial in-plane strain is defined as  $\eta_1 = \eta_2 = (a - a_0)/a_0$ , where  $a_0$  is the equilibrium in-plane lattice constant. In our study, we consider compressive inplane strains.

Calculations are performed using the mixed-basis pseudopotential method.[15] The norm-conserving pseudopotentials are generated according to the Troullier-Martins procedure.[16] Atomic configurations for generating pseudopotentials, pseudo/all-electron matching radii, and accuracy checking were given elsewhere[17]. The wave functions of single-particle Kohn-Sham states in solids are expanded in terms of a basis set which consists of the linear combination of numerical atomic orbitals and plane waves. An energy cutoff of 100 Ryd is

used throughout all calculations for both bulk materials and superlattices, which we found sufficient for convergence.

In ferroelectric crystals with tetragonal symmetry, the polarization is nonzero along the out-of-plane  $c$  axis. Polarizations are calculated using the geometric phase of the valence manifold of electron wave functions according to the modern theory of polarization[18, 19], which we have implemented in our mixed-basis computational scheme.

### III. RESULTS

#### A. Structure and polarization under zero strain

To better understand the strain effects in PT/ST and BT/ST superlattices, we first study the equilibrium structure of the superlattices under zero external strain. By minimizing the total energy of these superlattices, we obtain that the unstrained superlattices have an optimized inplane lattice constant  $a=3.87\text{\AA}$  and tetragonality  $c/a=2.0$  for PT/ST, and  $a=3.91\text{\AA}$  and  $c/a=2.0$  for BT/ST. Comparing with our theoretical inplane lattice constants of unstrained pure bulk materials—which are  $a=3.88\text{\AA}$  for PT,  $a=3.95\text{\AA}$  for BT, and  $a=3.86\text{\AA}$  for ST, we thus see that, when transitioning from bulk to superlattices, the PT (or BT) layers are compressively strained while the ST layers are stretched.

For unstrained PT/ST and BT/ST superlattices, our calculations using the modern theory of polarization reveal that both superlattices have zero polarization, showing that the properties in the short-period superlattices differ significantly from bulk PT and BT constituents. The calculated vanishing polarization in the BT/ST superlattice does not contradict the experimental results[20] where the BT/ST superlattice with one unit cell of BT was found to be ferroelectric, since the experimental sample was grown on SrTiO<sub>3</sub> substrate with an inplane lattice constant of  $a=3.86\text{\AA}$ . In our case, the BT/ST superlattice is free standing without substrate ( $a=3.91\text{\AA}$ ). The null polarization in equilibrium PT/ST and BT/ST superlattices is interesting and meanwhile puzzling, if one recognizes that *bulk* PT has a very large polarization of  $\sim 65\mu\text{C}/\text{cm}^2$  when strained to  $a=3.87\text{\AA}$  (the inplane lattice constant of the PT/ST superlattice), and bulk BT also has a large polarization of  $\sim 35\mu\text{C}/\text{cm}^2$  when strained to  $a=3.91\text{\AA}$  (the inplane lattice constant of the BT/ST superlattice). One may wonder why the strained PT or BT layers inside the superlattices do not polarize the ST

layers and lead to some polarization.

To understand why the unstrained superlattices have null polarization, we examine the optimized atomic positions at zero strain, which is schematically shown in Fig.1(a). The  $z$ -axis is along the superlattice stacking direction, i.e., the direction of the tetragonal  $c$ -axis. Here we are interested in the relative atomic displacements, rather than the absolute shifts of each atom. By placing Pb at the origin, we define a high-symmetry location along the  $z$ -direction for each atom; more specifically, the high-symmetry locations for Sr and  $O'_1$  atoms are at  $z = \frac{c}{2}$ , while those of Ti and  $O'_2$  atoms are respectively located at  $z = \frac{c}{4}$  and  $z = \frac{3c}{4}$  along the  $z$ -axis. In Fig.1(b) we show the  $z$ -axis atomic displacements of the LDA-optimized structure with respect to the high-symmetry locations for different atoms. We see that the  $O_2$  and  $O'_2$  atoms undergo a notable displacement that is 0.6% of lattice length  $c$ . Meanwhile, the Ti atom (which shares the same plane as  $O_2$ ) is also displaced off the center of high symmetry, but the amount of displacement of Ti differs from that of  $O_2$ . As a result of the different displacements from Ti and  $O_2$ , our calculations thus reveal that there is a local dipole moment for the Ti- $O_2$  plane. However, due to the fact that  $O_2$  and  $O'_2$  atoms move along the opposite directions with equal amount of displacements (so do Ti and Ti'), the local dipole moments of the Ti- $O_2$  plane and Ti'- $O'_2$  plane thus cancel, leading to a vanishing total polarization. Since both  $O_2$  and  $O'_2$  shift towards Sr, the inversion symmetry by the SrO-plane is thus maintained (to the accuracy of numerical certainty). This explains why the superlattice has no polarization at zero strain.

The opposite displacements of  $O_2$  and  $O'_2$  can not be naively attributed to the size difference between Sr and Pb, since their numerical atomic sizes do not differ significantly. By analyzing the electron density for the optimized structure and for the high-symmetric structure, we found that  $O_2$  and  $O'_2$  move towards Sr because of the strong covalent bonding between O and Sr. This makes sense since the covalent nature of the Sr-O bond is stronger than that of Pb-O or Ba-O. It also implies that if one replaces Sr by other A-site atoms with less covalent nature, there may be a possibility to produce polarization. Our study thus shows that atoms in zero-strain superlattices indeed are displaced off the center, but the displacement pattern maintains the plane-inversion symmetry.

## B. Dependence of mixing energy on inplane strain

Thermodynamically, when constituents A and B form the A/B superlattice, the mixing energy is defined as

$$\Delta E(a) = E_{A/B}(a) - E_A(a) - E_B(a) \quad , \quad (1)$$

where  $E_{A/B}$  is the total energy of a 10-atom cell for the  $1 \times 1$  superlattice, while  $E_A$  (or  $E_B$ ) is the total energy of one unit cell of bulk material A (B). All energies are calculated at the same inplane  $a$  lattice constant, with the out-of-plane  $c$  lattice constant and atomic positions optimized for each structure involved in Eq.(1). Mixing energy tells us the relative stability of the superlattice with respect to the individual constituents. A positive mixing energy means that the superlattice is *thermodynamically* less stable and will segregate into pure constituents. Of course, this segregation may take a long time due to the possible existence of energy barrier. While polarization properties of FE superlattices have been studied, little is known thus far about the mixing energy, for instance, (i) What is the value of mixing energy for prototypical superlattice such as PT/ST or BT/ST? (ii) How does the change in the inplane strain affect the mixing energy?

Figure 2 shows the mixing energies  $\Delta E$ , as well as total energies  $E_{A/B}$  and  $E_A + E_B$ , for the PT/ST and BT/ST systems at different inplane lattice constants. From Fig.2, we find that, (i) For PT/ST, the mixing energy is always positive in the considered strain region, revealing that the superlattice is thermodynamically less stable as compared to segregated bulk constituents and an extra energy is needed to build the PT/ST superlattice. (ii) However, the BT/ST superlattice turns out to have a negative mixing energy at small strains, thus being thermodynamically stable energywise. (iii) When the inplane strain is small, the mixing energy  $\Delta E$  of PT/ST increases in a linear fashion with the decreasing  $a$  lattice constant. Interestingly, this increase does not last forever; instead  $\Delta E$  reaches its peak value at a certain inplane lattice and then starts to decline when  $a$  is further reduced. In fact, we have calculated  $\Delta E$  down to  $a=3.60\text{\AA}$  (not shown in the figure), which confirms the continuous decline of  $\Delta E$ . The non-monotonous strain dependence of the mixing energy is found true also for BT/ST. (iv) For the strain region considered, the mixing energy ranges from 20 to 100 meV per 10-atom cell for PT/ST, while for BT/ST it is within  $\pm 20$  meV. In other words, the mixing energy is large for PT/ST, while being rather close to zero for BT/ST. As a result of the small mixing energy, BT and ST are more likely to form FE

alloys, which is indeed true in experiments.

### C. Ferroelectric polarization

Previous studies on the ferroelectric polarization in superlattice largely focused on the case that the inplane lattice constant of the superlattice is fixed to be that of substrate  $\text{SrTiO}_3$ . Here, our emphasis is slightly different; we examine the polarization in superlattice under varied inplane lattice constants, and study how the superlattice responds differently (or similarly) to the inplane strain as compared to the bulk constituents. In Fig.3(a) we show the total (electronic+ionic) polarizations in PT/ST and BT/ST superlattices, in comparison with the values in bulk PT, BT, and ST. On the one hand, the result in Fig.3(a) is rather trivial—it shows that for a given inplane  $a$  lattice constant, polarization in BT/ST superlattice is larger than in ST, but smaller than in BT. As a result, polarization in BT/ST superlattice never exceeds that in bulk BT of the same  $a$ . Similar conclusion is also true for PT/ST. On the other hand, a careful examination of the calculation results in Fig.3(a) reveals some interesting observations: (1) At  $a_1=3.86\text{\AA}$  (which is the inplane lattice constant of typical substrate  $\text{SrTiO}_3$ ), BT/ST has a sizable polarization while PT/ST does not, although, at this  $a_1$  lattice constant, bulk PT has a much larger polarization than bulk BT. This suggests that, the concept that a stronger FE component (such as PT as compared to BT) in superlattice will polarize better the non-FE component (such as ST) does not always work. (2) Below and above  $a_2=3.82\text{\AA}$ , the polarization curve of PT/ST (similarly of BT/ST) undergoes an evident change in the slope. More specifically, the polarization rises more slowly when  $a < a_2$ , as compared to the case when  $a > a_2$ . We recognize that  $a_2$  actually coincides with the critical inplane lattice constant where bulk ST starts to become ferroelectric. The critical property of *bulk* ST (namely, becoming FE at  $a_2$ ) is thus also reflected in *superlattices*. As the ST component turns ferroelectric when  $a < a_2$ , PT/ST or BT/ST becomes less incipient, thus showing a smaller strain-induced polarization enhancement. (3) When  $a > a_2$ , polarization in PT/ST is smaller than in BT/ST. However, when  $a < a_2$ , a crossover occurs, and polarization in PT/ST becomes larger than in BT/ST.

When bulk constituents A and B form an A/B superlattice, one can use the polarizations



of bulk FEs and define an average of polarization

$$\bar{P}(a) = \frac{P_A(a)\Omega_A(a) + P_B(a)\Omega_B(a)}{\Omega_A(a) + \Omega_B(a)} \quad (2)$$

for a given inplane  $a$  lattice constant, where  $P_A$  and  $\Omega_A$  are the polarization and cell volume of the  $A$  constituent, respectively. This definition is based on the fact that polarization itself (namely, dipole moment per unit volume) is not an additive thermodynamic quantity and must be weighted by volume. We then compare the polarization  $P_{A/B}$  of the superlattice (calculated using optimized structure and modern theory of polarization) with  $\bar{P}$  by examining  $\Delta P = P_{A/B} - \bar{P}$ .  $\bar{P}$  can be viewed as the anticipated polarization when one combines bulk A and B constituents together into a heterostructure, each with the same inplane lattice constant  $a$ , but without interaction between them. The  $\Delta P$  quantity thus reflects mainly the interfacial effect on the polarization, caused by various interactions such as the polarizing (or depolarizing) field and size effect.

The  $\bar{P}$  and  $\Delta P$  quantities are given in Fig.3(b) for PT/ST and in Fig.3(c) for BT/ST. For PT/ST, we see in Fig.3(b) that (1) when  $a$  decreases,  $P$  of the superlattice increases faster than  $\bar{P}$ ; (2)  $\Delta P$  is negative in the strain range considered, namely the polarization of superlattice does not exceed  $\bar{P}$ ; (3) At small compressive strains,  $P_{A/B}$  and  $\bar{P}$  differ significantly. But at large compressive strains, they become close. For BT/ST in Fig.3(c),  $\Delta P$  is negative at small strains. However, when  $a < 3.84\text{\AA}$ ,  $\Delta P$  becomes positive, revealing that  $P$  of short-period superlattice can in fact exceed the average  $\bar{P}$  of bulk constituents. If we examine the magnitude of  $\Delta P$  (a quantity that indicates the gain of polarization when two materials form superlattice), we see that for PT/ST, the gain runs from  $-40 \mu\text{C}/\text{cm}^2$  to zero, while for BT/ST, the gain stays within  $\pm 10 \mu\text{C}/\text{cm}^2$ .

Generally one tends to think that polarization in superlattice is to be enhanced with respect to the average of single materials. This need be taken with caution. As shown in Fig.3(b) for PT/ST, the polarization of the superlattice is considerably smaller than the average  $\bar{P}$  of the corresponding single materials at the same inplane  $a$ ; while for BT/ST, the gain of polarization varies from negative to positive as strain increases. As an outcome of the competing effect between polarizing field and different covalent strengths of different A-site atoms, the gain of total polarization in the superlattice is thus a collective result influenced by the properties of single materials, their interaction, and external strain.

Technologically, one possible advantage of forming FE superlattices is to tune material

properties. Here we examine how piezoelectric coefficients may be tuned in PT/ST as compared to bulk PT. We are interested in the proper piezoelectric coefficient  $e_{31} = -\frac{e}{\Omega} \frac{d\chi}{d\eta_1} c$ , where  $\chi$  is related to the  $c$ -axis polarization by  $P_3 = \frac{e}{\Omega} \chi c$ .  $e_{31}$  reflects what magnitude of polarization enhancement can be achieved by applying the inplane strain  $\eta_1$ . In Fig.3(d) we show the  $\chi$  polarizations in PT/ST and in bulk PT. Fitting the  $\chi$  values over the considered strain range yields piezoelectric coefficient  $e_{31}$ , and the resulting  $e_{31}$  values are given near the fitting lines in Fig.3(d). One sees that, the piezoelectric  $e_{31} = 19.1 C/m^2$  coefficient in PT/ST is much larger than the value  $e_{31} = 10.6 C/m^2$  in bulk PT.

#### D. Microscopic insight: atomic displacements

To understand microscopically how different layers in superlattices interact and how they collectively respond to inplane strains, we report and analyze in this section the atomic displacements occurring in different layers of the superlattices.

Bulk ferroelectric perovskite  $ABO_3$  of tetragonal symmetry consists of two layers—the AO layer and the  $BO_2$  layer—alternating along the  $c$ -axis. The total electric polarization of the solid could be viewed as the local dipole contributions from the two individual layers, as demonstrated by the Wannier functions and local polarizations in Ref.21. The relative displacements of the A and B atoms with respect to the oxygen centers of the same layer are thus important quantities that reveal the origin and amplitude of the polarization in the material. In  $1 \times 1$  PT/ST superlattice, there are four non-equivalent atomic layers, namely, the Pb- $O_1$ , Ti- $O_2$ , Sr- $O'_1$  and Ti'- $O'_2$  layers (see Fig.1a). For the convenience of discussion, we define the  $z$ -direction relative displacement of the cation with respect to that of oxygen in each layer as  $\Delta z(PbO_1) = z(Pb) - z(O_1)$ ,  $\Delta z(TiO_2) = z(Ti) - z(O_2)$ ,  $\Delta z(SrO'_1) = z(Sr) - z(O'_1)$ , and  $\Delta z(Ti'O'_2) = z(Ti') - z(O'_2)$ , where  $z(A)$  is the  $z$ -axis position of atom A.  $\Delta z$ 's in the theoretically optimized structures of PT/ST and BT/ST are shown in Fig.4, where the corresponding displacements in pure bulk materials are also given for comparison.

Let us look at PT/ST first. It is known in bulk  $PbTiO_3$  that Pb has a considerable off-center displacement. As a result,  $PbTiO_3$  is a rather strong A-site FE. In comparison, bulk  $SrTiO_3$  has less ferroelectricity from the A-site. This is indeed confirmed by our calculation results of  $\Delta z(AO)$  for bulk PT and ST (see the dotted lines in Fig.4a). However, in PT/ST

superlattice, the  $\Delta z$  displacements are remarkably close for the Pb-O<sub>1</sub> layer and for the Sr-O<sub>1</sub>' layer (see two solid lines in Fig.4a). Also note that  $\Delta z(\text{SrO}_1')$  in PT/ST superlattice is much larger than the counterpart in bulk SrTiO<sub>3</sub>, for a fixed inplane lattice constant. These results are interesting and tell us that, by forming a superlattice, the SrTiO<sub>3</sub> component becomes a much stronger A-site FE, as compared to bulk ST. Regarding  $\Delta z(\text{PbO}_1)$  [or similarly  $\Delta z(\text{SrO}_1')$ ], we further recognize that this quantity should be identical to zero if the  $1 \times 1$  superlattice has a mirror inversion symmetry by a plane perpendicular to the  $c$ -axis. On the other hand, once the inversion symmetry is broken by the appearance of ferroelectricity,  $\Delta z(\text{PbO}_1)$  becomes nonzero. This is indeed verified by our numerical results in Fig.4(a), where  $\Delta z(\text{PbO}_1)$  is zero for  $a > 3.86\text{\AA}$  and nonzero for  $a < 3.86\text{\AA}$ . We thus see that  $\Delta z(\text{PbO}_1)$  serves as a *microscopic* order parameter for ferroelectricity in the  $1 \times 1$  superlattice. And this microscopic order parameter can be probed using x-ray diffraction since it is atomic displacement rather than electrical polarization.

In Fig.4(b) we examine the Ti relative displacements,  $\Delta z(\text{TiO}_2)$  and  $\Delta z(\text{Ti}'\text{O}_2')$ , with respect to oxygen in PT/ST. Unlike the A cations where  $\Delta z(\text{PbO}_1)$  and  $\Delta z(\text{SrO}_1')$  are almost identical in different layers, the Ti-O relative displacements in two TiO<sub>2</sub> layers are evidently different in Fig.4b. At zero strain ( $a=3.87\text{\AA}$ ), since the O<sub>2</sub> atom moves up and the O<sub>2</sub>' atom moves down due to the fact that the Sr-O bond has a stronger covalent nature than the Pb-O bond as described in a previous section (see Fig.1a),  $\Delta z(\text{TiO}_2)$  and  $\Delta z(\text{Ti}'\text{O}_2')$  appear to be equal but with opposite sign. With increasing strain, the O<sub>2</sub> atom starts to move downwards as ferroelectricity is developed, which causes  $\Delta z(\text{TiO}_2)$  to change from negative to positive in Fig.4a. Interestingly, even for very large inplane strains (e.g., at  $a=3.75\text{\AA}$ ), the difference between  $\Delta z(\text{TiO}_2)$  and  $\Delta z(\text{Ti}'\text{O}_2')$  still exists, showing that the stronger covalent nature of Sr-O bond continues to manifest itself in the microscopic picture.

From Fig.4(a) and (b), one thus sees that, even at large compressive inplane strains, the relative atomic displacements in PT/ST are considerably smaller than the counterparts in bulk PT, and meanwhile much larger than in bulk ST. This demonstrates the strong influence between two constituents when they form superlattice. On the other hand, within the PT/ST superlattice, atomic displacements are rather uniform in different layers, except for the slight difference in Ti-O displacements caused by the different covalency in A sites.

We next examine the situation in BT/ST as shown in Fig.4(c) and (d). At small strain in Fig.4(c), the relative displacements of Ba-O<sub>1</sub> and Sr-O<sub>1</sub>' are small and similar. As strain

increases, the difference increases. This is in difference from what we have previously seen in PT/ST where  $\Delta z(PbO_1)$  and  $\Delta z(SrO'_1)$  are close over a wide range of considered strains. The difference could be attributed to the large size of Ba atom which, as the inplane  $a$  constant decreases, will push away more strongly the oxygen atom on the BaO plane, leading to a larger difference in  $\Delta z(BaO_1)$  than in  $\Delta z(SrO'_1)$ . Regarding the Ti-O displacement in BT/ST, we see in Fig.4(d) that, as compressive strain increases,  $\Delta z(TiO_2)$  and  $\Delta z(Ti'O'_2)$  become gradually close to each other. At  $a=3.75\text{\AA}$ ,  $\Delta z(TiO_2)$  exceeds  $\Delta z(Ti'O'_2)$ , showing a crossover that does not occur in PT/ST.

### E. Effective charges

In this part of the section we study how the effective charges of atoms are modified when forming superlattices. For each inplane lattice constant, we compute the effective  $Z_{33}^*$  by finite difference  $Z_{33}^* = \frac{\Omega \Delta P}{e \Delta r_z}$ , where  $\Delta r_z$  is chosen to be  $0.002c$ . All effective charges are given in unit of one electron charge.

For equilibrium structures of zero strain, the calculated effective charges in superlattices and in bulk materials (each at its own equilibrium) are given in Table I. The most notable results in Table I are: (i)  $Z_{33}^*$  of Ti atom in bulk PT is merely 5.76. However, its value drastically increases to 7.31 in the PT/ST superlattice. Therefore,  $Z^*$ s in bulk materials can not and should not been used in superlattices. In bulk PT, the Ti atom is strongly bonded to only one of the nearby  $O_1$  atoms due to the strong tetragonality. In PT/ST, the Ti atom is bonded to both  $O_1$  and  $O'_1$ , leading to a large  $Z_{33}^*$ . (ii) while  $Z_{33}^*$ s of the A, Ti, or  $O_1$  sites change significantly from bulk to superlattice,  $Z_{33}^*$ s of the  $O_2$  site are similar in bulk and in superlattice. (iii) In PT/ST at equilibrium,  $Z^*$ s of two non-equivalent Ti atoms, namely  $Z_{33}^*(Ti)$  and  $Z_{33}^*(Ti')$ , are identical, so are  $Z_{33}^*(O_2)$  and  $Z_{33}^*(O'_2)$ . This is caused by the planar inversion symmetry in equilibrium structure. Similar conclusion is true for BT/ST except for some numerical uncertainty. (iv) In PT/ST,  $Z_{33}^*$ s of two non-equivalent  $O_1$  atoms—i.e.,  $Z_{33}^*(O_1)$  and  $Z_{33}^*(O'_1)$ —are very different. The  $O'_1$  atom on the SrO layer has a much larger  $Z_{33}^*$  than the  $O_1$  atom on the PbO layer.

Under the application of strain, effective charge for each atom is given in Fig.5(a) for PT/ST. First, we see that, as the inplane lattice constant decreases by  $0.14\text{\AA}$ , the effective charge of Ti atom decreases sharply from 7.31 at  $a=3.88\text{\AA}$  to  $\sim 4.50$  at  $a=3.74\text{\AA}$ , demon-

strating a wide range of tunability. Similar scale of tunability also occurs to the  $O_1$  and  $O'_1$  atoms. In contrast, the  $Z_{33}^*$  charges of Pb, Sr,  $O_2$  and  $O'_2$  atoms subject to relatively small changes (around 0.3). Second, under compressive inplane strains, the  $Z_{33}^*$  charges of the  $O_2$  and  $O'_2$  atoms are no longer identical, unlike the zero-strain case. At zero strain, the  $O_2$  and  $O'_2$  atoms are symmetric due to the planar inversion symmetry. Under compressive strains, the symmetry between  $O_2$  and  $O'_2$  is broken as ferroelectricity develops. Meanwhile, the Ti- $O_1$  bond is considerably weakened as a result of the increasing tetragonality, which is responsible for the sharp decline of  $Z_{33}^*(Ti)$ . Third, we recognize that the absolute magnitude of the  $Z_{33}^*$  charge decreases for most of atoms such as Pb, Ti,  $O_1$  and  $O_2$ , once the impressive strain is applied. One exception is Sr. As  $a$  decreases,  $Z_{33}^*$  of Sr increases instead, probably due to the strain strengthened Sr- $O'_2$  bond. Many of these conclusions are also true for the effective charges in BT/ST which are shown in Fig.5(b), except for two evident differences: (1) As  $a$  decreases,  $Z_{33}^*$  of Ba increases, unlike Pb; (2)  $Z_{33}^*(O_2)$  and  $Z_{33}^*(O'_2)$  in BT/ST are very similar over the considered strain range.

## F. Polarization structure

Polarization structure [13] reveals how the geometrical phase  $\phi(\vec{k}_\perp)$  of individual  $\vec{k}_\perp$  string contributes to the electronic polarization  $\vec{P}_{el}$ , as described by the modern theory of polarization[18, 19] in the equation  $\vec{P}_{el} = \frac{2e}{(2\pi)^3} \int d\vec{k}_\perp \phi(\vec{k}_\perp)$ , where  $\phi(\vec{k}_\perp) = i \sum_{n=1}^M \int_0^{G_\parallel} dk_\parallel \langle u_{n\vec{k}} | \frac{\partial}{\partial k_\parallel} | u_{n\vec{k}} \rangle$ . Like band structure, the  $\phi(\vec{k}_\perp) \sim \vec{k}_\perp$  polarization structure contains various important microscopic insight into the polarization properties. Furthermore, it was shown that the polarization structure is determined by, and thus can reveal, the fundamental interaction among Wannier functions.[13] While the  $\phi(\vec{k}_\perp) \sim \vec{k}_\perp$  dispersion of bulk ferroelectric has been studied previously,[13] the polarization structure of FE superlattices remains interesting and unknown. For instance, when bulk BT and ST form BT/ST superlattice, the *total* polarization is known (Fig.3a) to decline as compared to bulk BT. However, it is not clear at which  $\vec{k}_\perp$  points the  $\phi(\vec{k}_\perp)$  phases suffer more; will the  $\vec{k}_\perp$  points near the zone center or near the zone boundary suffer most? Also, how is the polarization dispersion in superlattice to be affected by the inplane strain?

The polarization structures of the BT/ST superlattice at two different inplane lattice constants,  $a=3.86\text{\AA}$  and  $a=3.82\text{\AA}$ , are shown in Fig.6, where the counterpart polarization

structures of bulk BT and ST at the same  $a$  length are also made available for comparison. Our calculation results in Fig.6a show that, at  $a=3.86\text{\AA}$ , the band width of the polarization structure in BT/ST is far smaller than that in BT. When transitioning from BT to BT/ST, the reduction of the  $\phi(\vec{k}_\perp)$  phase occurs mainly near the  $X_1$  and  $X_2$  points. In other words, the  $\phi(\vec{k}_\perp)$  phases near the zone boundary are most affected when forming FE superlattices.

Based on the consideration that (1) bulk BT and bulk ST have very different polarization dispersion at a fixed  $a$  lattice constant, and (2) the  $\phi(\vec{k}_\perp)$  phase is inversely proportional to the  $c$ -lattice length,[13] one valid approach to compare, at a given  $\vec{k}_\perp$  point, the  $\phi(\vec{k}_\perp)$  phases in superlattice with those in bulk constituents is to define an average phase as  $\bar{\phi}(\vec{k}_\perp, a) = \frac{1}{c_A(a)+c_B(a)}[\phi_A(\vec{k}_\perp, a)c_A(a) + \phi_B(\vec{k}_\perp, a)c_B(a)]$ , where  $c_i(a)$  is the  $c$ -lattice length of bulk  $i$  at the inplane lattice constant  $a$ , and  $c_{A/B}$  is the  $c$ -lattice length of the superlattice. All quantities in the above equation are calculated at the same  $a$  lattice constant.  $\bar{\phi}$  is also depicted in Fig.6. At  $a=3.86\text{\AA}$ , we find that  $\phi(\vec{k}_\perp)$  in BT/ST can be described rather well by  $\bar{\phi}$ . However, this is not the case for  $a=3.82\text{\AA}$ . In Fig.6b, one sees: (i) Though bulk ST still has zero polarization with  $\phi(\vec{k}_\perp)=0$  for all  $\vec{k}_\perp$  strings, the  $\phi(\vec{k}_\perp)$  dispersion in the BT/ST superlattice is nevertheless notably similar to that of bulk BT. (ii)  $\phi(\vec{k}_\perp)$  in BT/ST is considerably larger than the average  $\bar{\phi}$  phase, demonstrating that the strong interaction between the BT layer and the ST layer makes the BT/ST superlattice no longer resembling the average of two bulk materials. The strong interaction takes place at  $a_2=3.82\text{\AA}$  but not at  $a_1=3.86\text{\AA}$ , since  $\text{SrTiO}_3$  at  $a_2$  is near the critical point of becoming ferroelectric, and can thus be easily polarized by the electric field arising from the polarization in the  $\text{BaTiO}_3$  layer.

#### IV. SUMMARY

Density-functional calculations were performed to study a variety of properties in  $1\times 1$   $\text{PbTiO}_3/\text{SrTiO}_3$  and  $\text{BaTiO}_3/\text{SrTiO}_3$  superlattices of tetragonal symmetry under compressive inplane strains. An emphasis is placed on the side-by-side comparison of these properties in superlattices and in bulks, which is particularly useful in terms of obtaining insight into the rather complicated interplay between inplane strains and interface effects. The investigated properties include equilibrium structure, strain dependence of mixing energy, ferroelectric polarization, microscopic atomic displacements, effective charges, and dispersion of

polarization structure. Our main findings are summarized in the following.

(i) In zero-strain superlattices without oxygen rotation, while atoms are indeed displaced off the centers, the displacements nevertheless maintain a plane inversion symmetry. As a result, the superlattices show no polarization. The planar inversion symmetry (and thus the vanishing polarization) in zero-strain superlattices originates from the strong covalent bonding between Sr and O. (ii) The mixing energy is found small and on the order of 20 meV for the BT/ST superlattice. For PT/ST, this mixing energy is relatively large and ranges from 20 to 100 meV in the considered strain region. The small mixing energy in BT/ST is consistent with the fact that BT and ST are more likely to form ferroelectric alloys. (iii) Under *small* inplane strains, the mixing energy is revealed to increase linearly with the decreasing inplane lattice constant. However, at a certain (large) inplane strain, the mixing energy starts to decline with the decreasing inplane  $a$  lattice constant (Fig.2). As a result, the mixing energy  $\Delta E$  exhibits a non-monotonous behavior.

On ferroelectric polarization under strains, our calculations show: (iv) At the inplane lattice constant of SrTiO<sub>3</sub> substrate ( $a_1=3.86\text{\AA}$ ), BT/ST has a sizeable polarization while PT/ST does not, although at this  $a_1$  lattice constant bulk PT has a much larger polarization than bulk BT. This indicates that a stronger FE constituent (such as PT with respect to BT) does not always polarize better the non-FE component in short-period superlattices. (v) At  $a_2=3.82\text{\AA}$ , the polarization-vs- $a$  curve undergoes an evident change in slope for both PT/ST and BT/ST superlattices, due to the fact that the incipient ST component starts to turn ferroelectric. For both superlattices, the polarization rises more slowly when  $a < a_2$ , as compared to the region when  $a > a_2$ . (vi) The polarization in PT/ST is smaller than in BT/ST, when  $a > a_2$ . But for  $a < a_2$ , a crossover occurs, and the polarization in PT/ST becomes stronger than in BT/ST. (vii) By defining the average polarization  $\bar{P}$  using the values of spontaneous polarizations in bulks, we find that  $\Delta P = P_{A/B} - \bar{P}$  is negative for PT/ST in a wide range of considered inplane strains, revealing that the polarization in  $1\times 1$  PT/ST superlattice does not exceed the average polarization  $\bar{P}$  of bulks. On the other hand, for BT/ST,  $\Delta P$  is found becoming positive when  $a < 3.84\text{\AA}$ .  $\Delta P$  ranges from -40 to 0  $\mu\text{C}/\text{cm}^2$  for PT/ST, and varies within  $\pm 10 \mu\text{C}/\text{cm}^2$  for BT/ST. (viii) The piezoelectric  $e_{31}$  coefficient of PT/ST is calculated to be 19.1  $\text{C}/\text{m}^2$ , much larger than the value of 10.6  $\text{C}/\text{m}^2$  of bulk PT.

Regarding the atomic displacements in PT/ST superlattice, our study reveals that (ix)

in  $1 \times 1$  superlattice of tetragonal symmetry,  $\Delta z(PbO_1)$  or  $\Delta z(SrO'_1)$  acts like a microscopic order parameter for the appearance of ferroelectricity. Since this order parameter is the change in atomic positions, it can thus be probed using x-ray diffraction. (x) The relative atomic displacements  $\Delta z(PbO_1)$  and  $\Delta z(SrO'_1)$  in PT/ST are found to be very close, over a wide range of inplane strains. The large values in our calculated  $\Delta z(SrO'_1)$  indicate that, by forming superlattices with PT, the ST component in PT/ST becomes a rather strong A-site FE as compared to bulk ST. (xi) The Ti-O displacements  $\Delta z(TiO_2)$  and  $\Delta z(Ti'O'_2)$  in PT/ST differ, however, owing to the fact that  $O_2$  and  $O'_2$  atoms have a tendency to move in opposite directions in order to form stronger covalent bonds with the Sr atom. Calculation results further show that this tendency continues to manifest itself even at very large inplane strains. (xii) For a given inplane lattice constant, the atomic displacements in bulk PT and bulk ST are considerably different. However, after PT and ST form a superlattice, the displacements in adjacent PT and ST layers are rather uniform, demonstrating the strong influence between two constituents. (xiii) In BT/ST superlattice, since Ba and Sr atoms have different sizes,  $\Delta z(BaO_1)$  and  $\Delta z(SrO'_1)$  deviate significantly from each other at high inplane strains.

On effective charges, the calculation results tell us: (xiv) in PT/ST under zero strain,  $Z_{33}^*$  of Ti is 7.31, much larger than  $Z_{33}^*=5.76$  in bulk PT. Furthermore,  $Z_{33}^*$ s of  $O_1$  and  $O'_1$  in PT/ST are found to be very different, more specifically,  $Z_{33}^*(O_1)=-5.36$  and  $Z_{33}^*(O'_1)=-6.38$ . (xv) With application of increasing inplane strains, the magnitude of  $Z_{33}^*$  drastically decreases for Ti and  $O_1$  atoms, showing a wide range of tunability. Meanwhile, as  $a$  decreases,  $|Z_{33}^*|$  of Sr is shown to increase whereas  $|Z_{33}^*|$ s of Pb, Ti,  $O_1$  and  $O_2$  atoms all decrease.

Finally, the investigation on the polarization dispersion structure demonstrates (xvi) when bulks BT and ST form the BT/ST superlattice, it is the  $\phi(\vec{k}_\perp)$  phases near the zone boundary that are most affected. (xvii) At  $a=3.86\text{\AA}$ , the  $\phi(\vec{k}_\perp)$  phase in BT/ST is revealed to be much smaller than the  $\phi(\vec{k}_\perp)$  phase in bulk BT of the same  $a$ , and is quantitatively close to the averaged  $\bar{\phi}$  phase. (xviii) However, at  $a=3.82\text{\AA}$ , the  $\phi(\vec{k}_\perp)$  phase in BT/ST superlattice is interestingly similar to that of bulk BT, despite the fact that bulk ST still shows no polarization at this inplane lattice constant. Furthermore, our calculations show that, when bulk ST is near the critical point of becoming ferroelectric, the strong interaction between the  $BaTiO_3$  layer and the  $SrTiO_3$  layer makes the  $\phi(\vec{k}_\perp)$  dispersion in BT/ST no longer resembling the average  $\bar{\phi}$  phase.



## ACKNOWLEDGMENTS

This work was supported by the Office of Naval Research.

---

- [1] M.E. Lines and A.M. Glass, Principles and applications of ferroelectrics and related materials (Clarendon, Oxford, 1979).
- [2] J. B. Neaton and K. M. Rabe, Appl. Phys. Lett. **82**, 10(2003).
- [3] M. Dawber, K. M. Rabe, and J. F. Scott, Rev. Mod. Phys. **77**, 1083 (2005).
- [4] K. J. Choi, M. Biegalski, Y. L. Li, A. Sharan, J. Schubert, R. Uecker, P. Reiche, Y. B. Chen, X. Q. Pan, V. Gopalan, L.-Q. Chen, D. G. Schlom, and C. B. Eom, Science **306**, 1005 (2004).
- [5] C. Ederer and N. A. Spaldin, Phys. Rev. Lett. **95**, 257601 (2005).
- [6] H. N. Lee, S. M. Nakhmanson, M. F. Chisholm, H. M. Christen, K. M. Rabe, and D. Vanderbilt, Phys. Rev. Lett. **98**, 217602 (2007).
- [7] Y. Yao and H. Fu, Phys. Rev. B **80**, 035126 (2009).
- [8] E. Bousquet, M. Dawber, N. Stucki, C. Lichtensteiger, P. Hermet, S. Gariglio, J.-M. Triscone, and P. Ghosez, Nature (London) **452**, 732 (2008).
- [9] M. Fornari and D. J. Singh, Phys. Rev. B **63**, 092101 (2001).
- [10] A. Garcia and D. Vanderbilt, Phys. Rev. B **54**, 3817 (1996).
- [11] K. Johnston, X. Huang, J. B. Neaton, and K. M. Rabe, Phys. Rev. B **71**, 100103 (2005).
- [12] L. Kim, J. Kim, U. Waghmare, D. Jung, and J. Lee, Phys. Rev. B **72**, 214121 (2005).
- [13] Y. Yao and H. Fu, Phys. Rev. B **79**, 014103 (2009).
- [14] P. Hohenberg and W. Kohn, Phys. Rev. **136**, B864 (1964); W. Kohn and L. J. Sham, Phys. Rev. **140**, A1133 (1965).
- [15] H. Fu and O. Gulseren, Phys. Rev. B **66**, 214114 (2002).
- [16] N. Troullier and J.L. Martins, Phys. Rev. B **43**, 1993 (1991).
- [17] Details of Pb, Ti, and O pseudopotentials were described in Ref.15. Configuration  $5s^25p^65d^{0.2}$  and matching radii  $r^{s,p,d}=2.0\text{Bohr}$  are used for Ba; configuration  $4s^24p^64d^{0.1}$  and matching radii  $r^{s,p,d}=1.50, 1.50, 2.0$  Bohr are used for Sr.
- [18] R. D. King-Smith and D. Vanderbilt, Phys. Rev. B **47**, 1651 (1993).
- [19] R. Resta, Rev. Mod. Phys. **66**, 889 (1994).

- [20] D. A. Tenne, A. Bruchhausen, N. D. Lanzillotti-Kimura, A. Fainstein, R. S. Katiyar, A. Cantarero, A. Soukiassian, V. Vaithyanathan, J. H. Haeni, W. Tian, D. G. Schlom, K. J. Choi, D. M. Kim, C. B. Eom, H. P. Sun, X. Q. Pan, Y. L. Li, L. Q. Chen, Q. X. Jia, S. M. Nakhmanson, K. M. Rabe, and X. X. Xi, *Science* **313**, 1614 (2006).
- [21] X. Wu, M. Stengel, K. M. Rabe, and D. Vanderbilt, **101**, 087601 (2008).

TABLE I: Effective charges  $Z_{33}^*$  of atoms in PT/ST superlattice (the 2nd column), in BT/ST superlattice (the 3rd column), and in bulk PT, BT, and ST (the 4th-6th columns). In  $1 \times 1$  superlattice, each site has two non-equivalent atoms. Each system is in its own equilibrium under zero strain.

atoms	PT/ST		BT/ST		PT	BT	ST
A site	3.32 (Pb)	2.91 (Sr)	2.75 (Ba)	2.57 (Sr)	3.65	2.79	2.56
Ti site	7.31 (Ti)	7.31 (Ti')	7.45 (Ti)	7.44 (Ti')	5.76	7.02	7.32
O <sub>1</sub> site	-5.36 (O <sub>1</sub> )	-6.38 (O' <sub>1</sub> )	-5.65 (O <sub>1</sub> )	-6.10 (O' <sub>1</sub> )	-4.90	-5.61	-5.77
O <sub>2</sub> site	-2.28 (O <sub>2</sub> )	-2.28 (O' <sub>2</sub> )	-2.22 (O <sub>2</sub> )	-2.21 (O' <sub>2</sub> )	-2.28	-2.13	-2.06

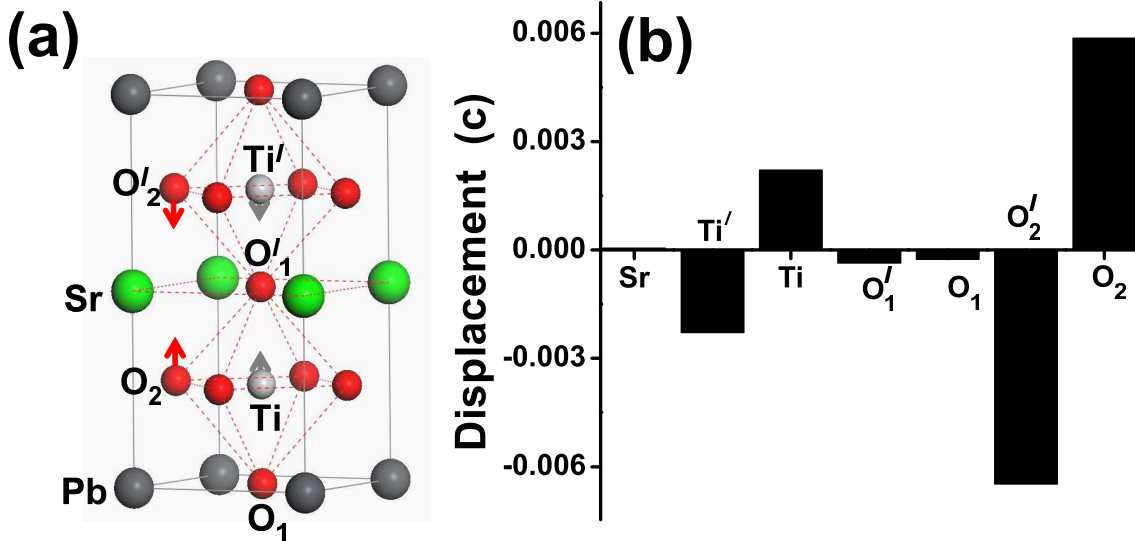


FIG. 1: (a) Schematic illustration of atomic positions and the direction of atomic displacements (by arrows) in the  $\text{PbTiO}_3/\text{SrTiO}_3$  superlattice at equilibrium. Individual atoms are labeled, for the sake of convenience of discussion. (b) Atomic displacements in the LDA-optimized structure with respect to the positions of high-symmetry. The displacements are in units of lattice constant  $c$ .

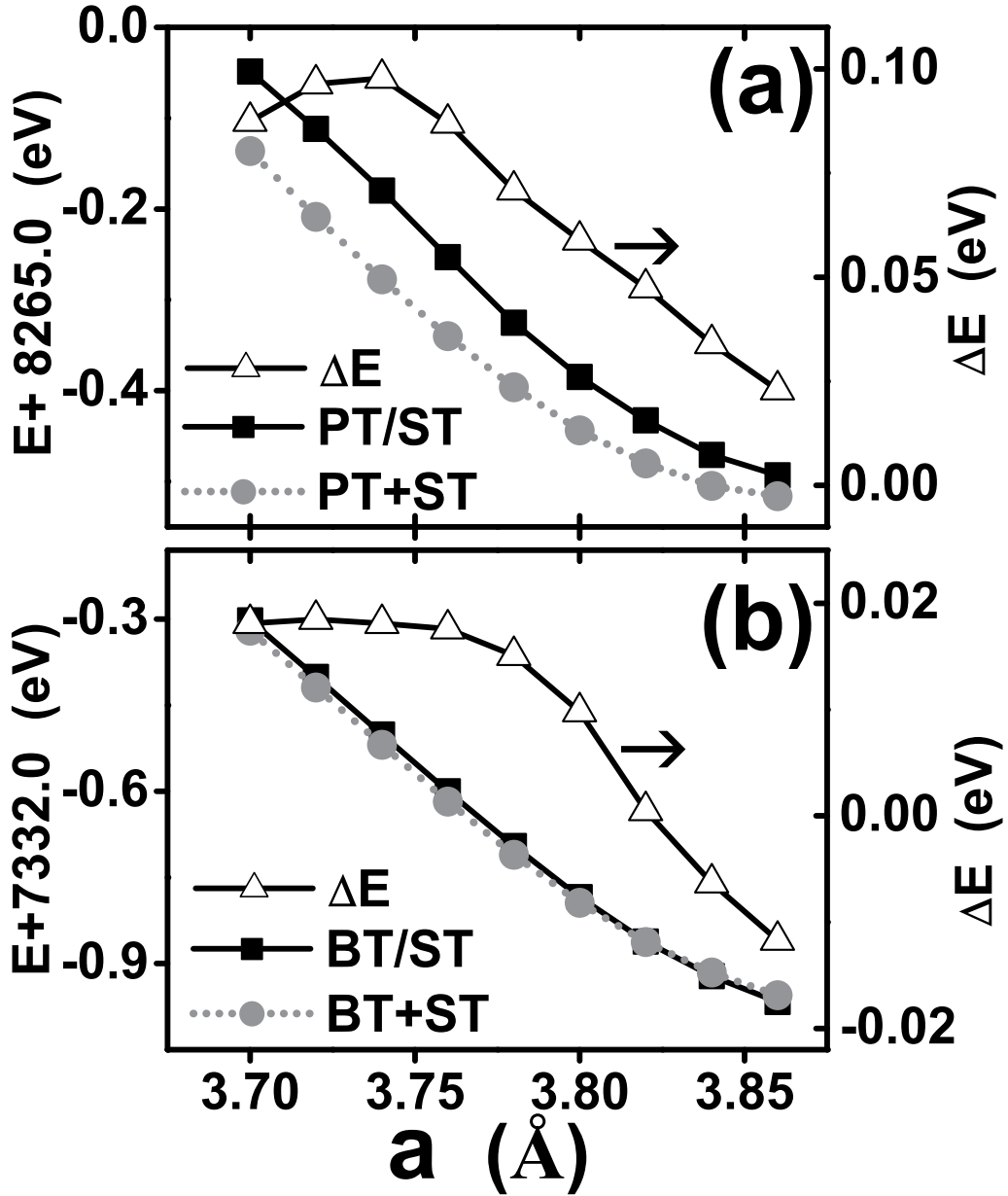


FIG. 2: (a) The total energy  $E_{A/B}$  of the superlattice (solid squares),  $E_A + E_B$  of the constituent bulks (solid dots), and the mixing energy  $\Delta E$  (empty triangles) as a function of the inplane lattice constant, for the PT/ST system.  $E_{A/B}$  and  $E_A + E_B$  are plotted using the left vertical axis, and  $\Delta E$  is plotted using the right vertical axis. Symbols are the calculation results; lines are guides for eyes. (b) The same as (a), but for the BT/ST system.

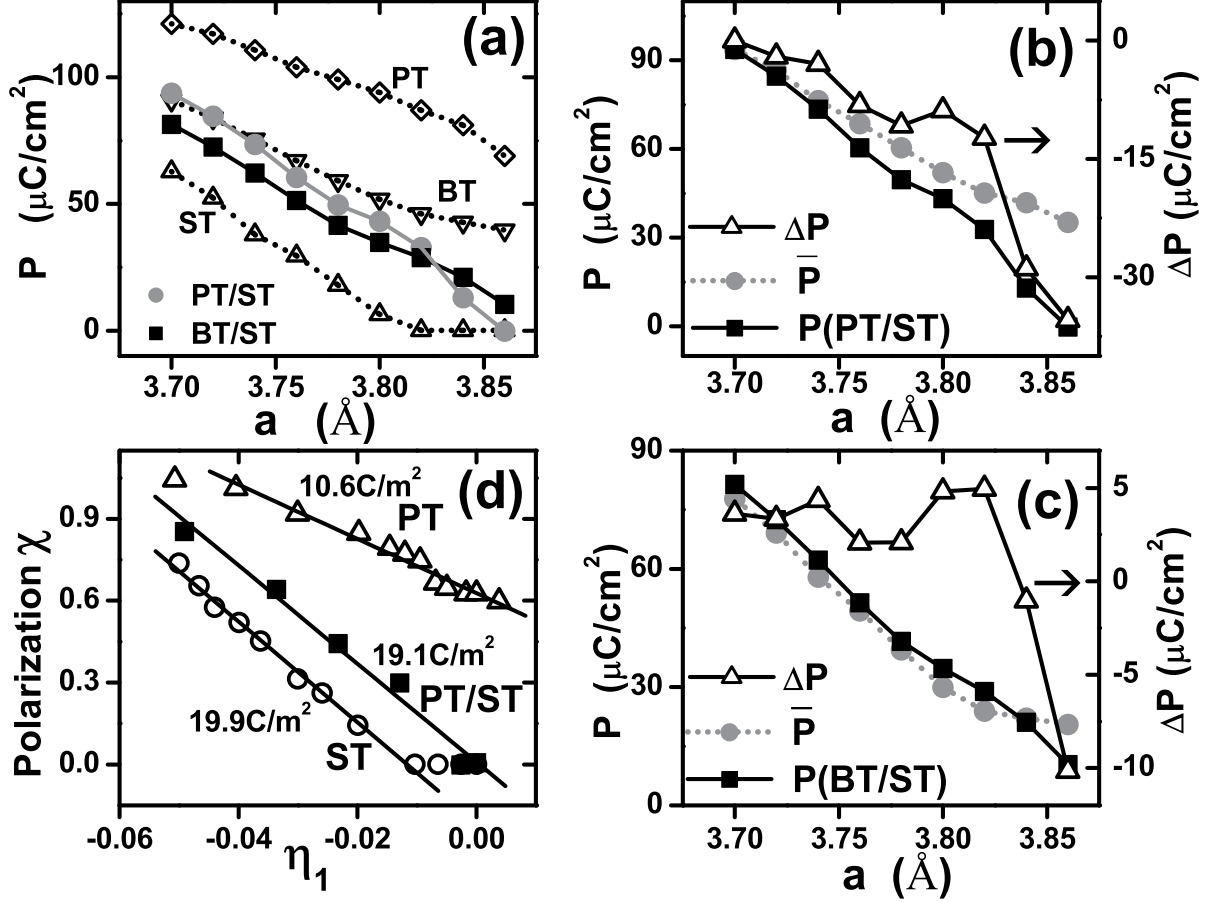


FIG. 3: (a) Total polarizations as a function of the inplane lattice constant, for PT/ST and BT/ST superlattices, as well as for bulk PT, BT, and ST. (b) Comparison between total polarization  $P$  (LDA-calculated) and average polarization  $\bar{P}$  (defined in Eq.2 using the polarizations of bulk materials), for the PT/ST system under different inplane  $a$  lattice constants. The difference  $\Delta P = P - \bar{P}$  is also shown.  $P$  and  $\bar{P}$  are plotted using the left vertical axis, and  $\Delta P$  is given using the right vertical axis. (c) The same as (b), but for the BT/ST system. In (a)-(c), symbols are the calculation results, and lines are guides for eyes. (d) The  $\chi$  polarizations as a function of the inplane  $\eta_1$  strain for superlattice PT/ST, bulk PT, and bulk ST. The numbers given near the fitting straight lines are the piezoelectric  $e_{31}$  coefficient.

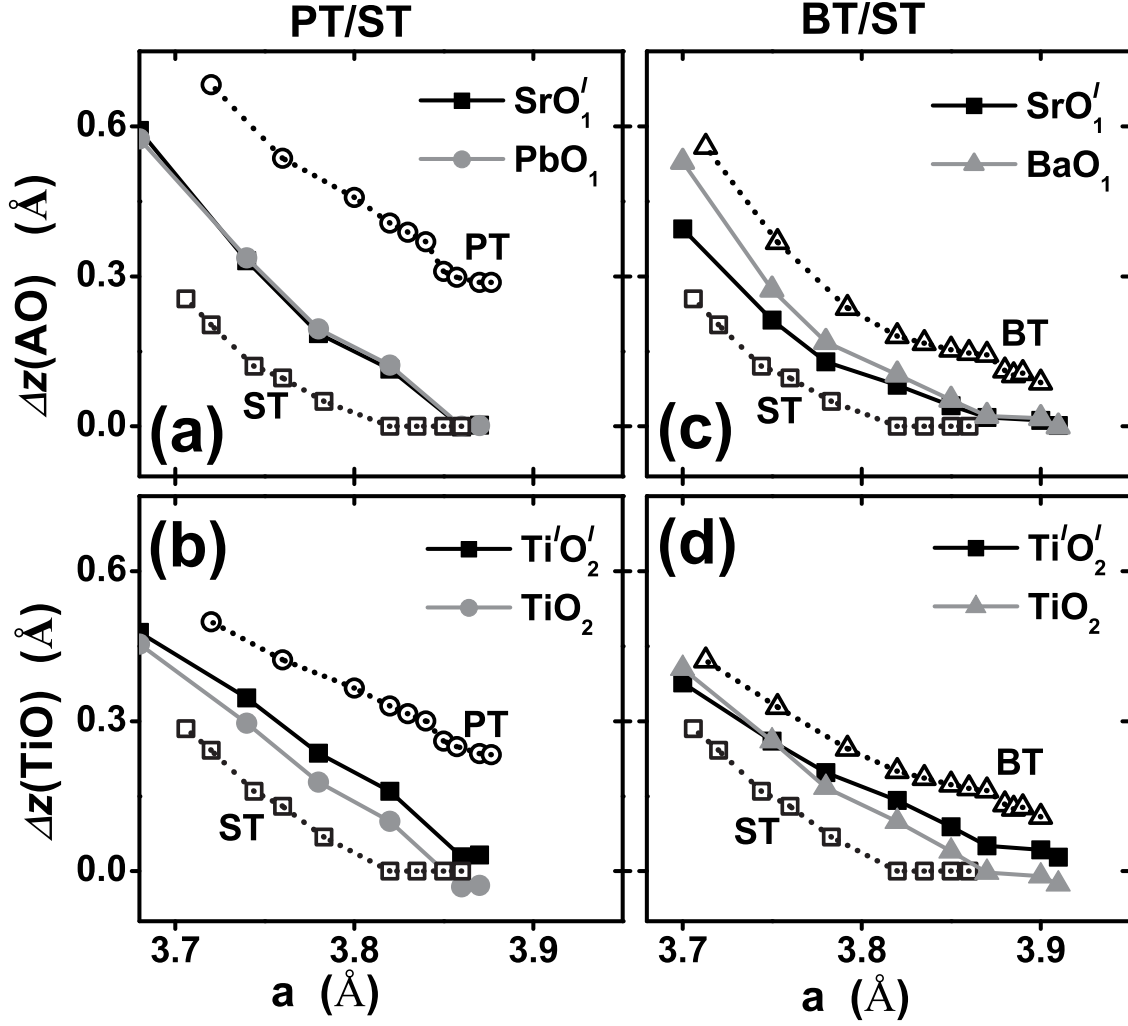


FIG. 4: Left panel: relative displacements for the PT/ST system; right panel: relative displacements for the BT/ST system. (a) Relative displacements  $\Delta z(PbO_1)$  and  $\Delta z(SrO'_1)$  in the PT/ST superlattice under different inplane lattice constants (the calculation results are depicted as the symbols on the solid lines). The counterpart displacements in bulk PT and in bulk ST under different lattice constants are also shown for comparison (by the symbols on the dotted lines). (b) Relative displacements  $\Delta z(TiO_2)$  and  $\Delta z(Ti'O'_2)$  in PT/ST under different inplane lattice constants (see the symbols on the solid lines). The counterpart displacements in bulk PT and in bulk ST are also shown (see the symbols on the dotted lines). (c) Similar as (a), but for the BT/ST superlattice. (d) Similar as (b), but for the BT/ST superlattice.

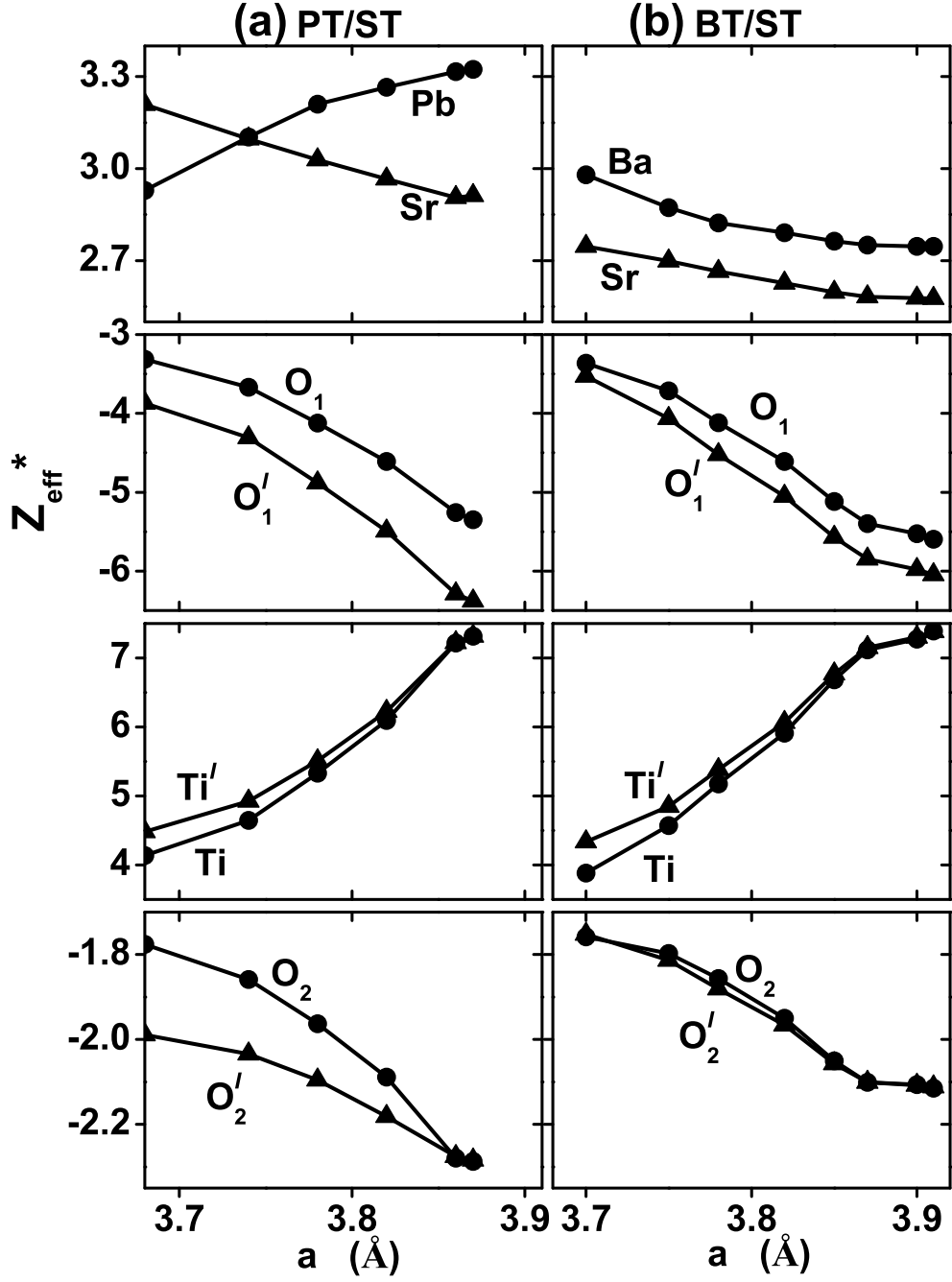


FIG. 5: Effective charges  $Z_{33}^*$  of the non-equivalent atoms in PT/ST superlattice (the left panel) and in BT/ST superlattice (the right panel), as a function of inplane lattice constant.

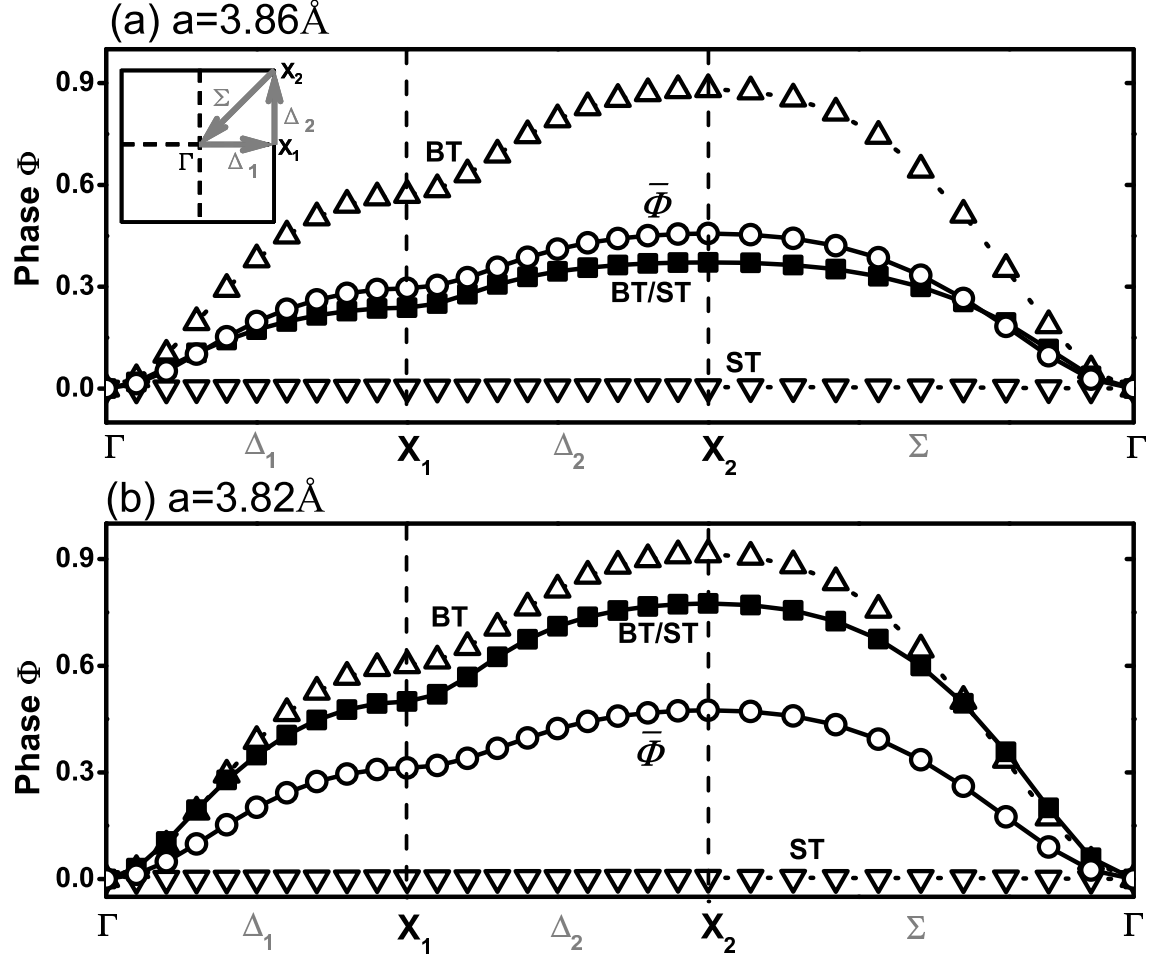


FIG. 6: (a) Polarization structures  $\phi(\vec{k}_\perp)$  of the BT/ST superlattice, bulk BT, and bulk ST, all at the same inplane lattice constant  $a=3.86\text{\AA}$ . The average  $\bar{\phi}$  phase (empty circles) is also shown for comparison. The  $\vec{k}_\perp$  plane of the Brillouin zone is shown as an inset. (b) Similar as (a), but for the inplane lattice constant  $a=3.82\text{\AA}$ .